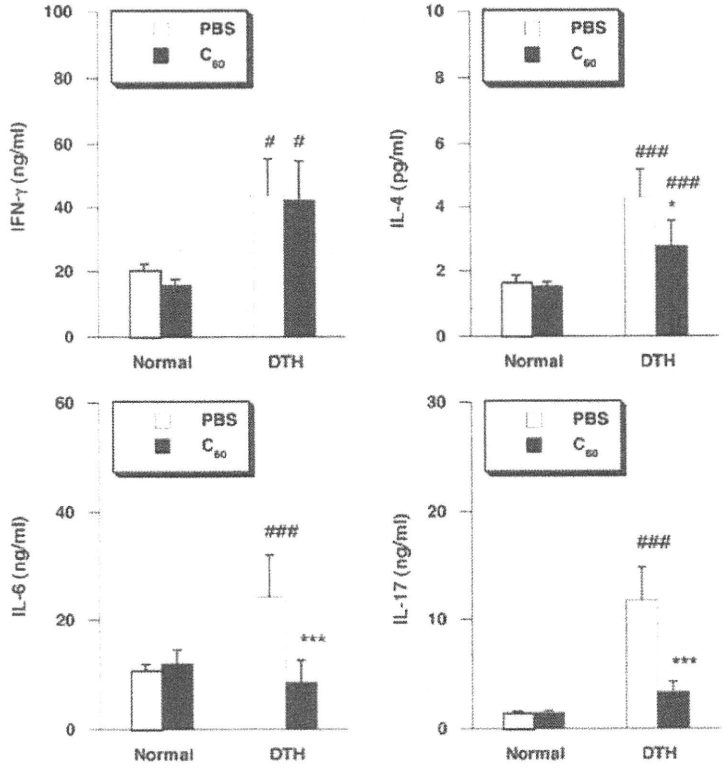

Fig. 3. Changes in cytokine production of splenocytes. Each value represents the mean ± S.E. ($n = 5$). DTH, delayed-type hypersensitivity; PBS, phosphate-buffered saline; C_{60}, nano-C_{60}. Statistically significant differences compared to the normal control group: $^{*}P < 0.05$, $^{***}P < 0.005$. Statistically significant differences compared to the DTH-disease control group: $^{\#}P < 0.05$, $^{\#\#\#}P < 0.005$.

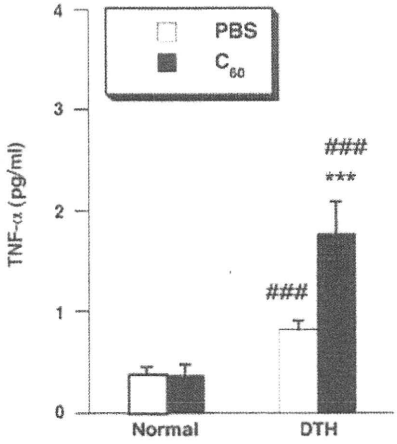

Fig. 4. Effect of nano-C_{60} treatment on the elevated TNF-α level observed in DTH-disease control mice. Each value represents the mean ± S.E. ($n = 5$). DTH, delayed type hypersensitivity; PBS, phosphate-buffered saline; C_{60}, nano-C_{60}. ***Statistically significant difference ($P < 0.005$) compared to the normal control group. $^{\#\#\#}$Statistically significant difference ($P < 0.05$) compared to the DTH-disease control group.

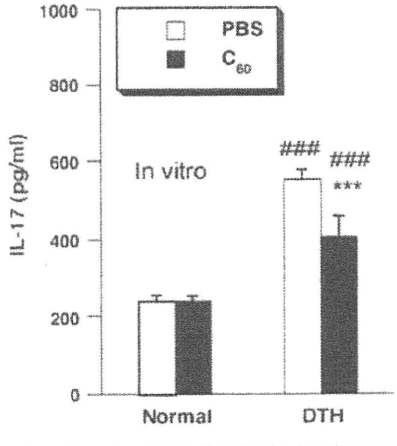

Fig. 5. Effect of nano-C_{60} on *in vitro* IL-17 production by splenocytes. Each value represents the mean ± S.E. ($n = 5$). PBS, phosphate-buffered saline; C_{60}, nano-C_{60}. ***Statistically significant difference ($P < 0.005$) compared to the normal control group. $^{\#\#\#}$Statistically significant difference ($P < 0.005$) compared to the DTH-disease control group.

4. Discussion

Fullerene acts as a photosensitizer, generating highly reactive singlet oxygen, which reacts with a wide range of biological targets, including lipids, proteins, nucleic acids and carbohydrates. This activity may prove to be an important constraint on its potential biomedical applications. We hypothesized that fullerene might exert adjuvant effects on the delayed hypersensitivity response of

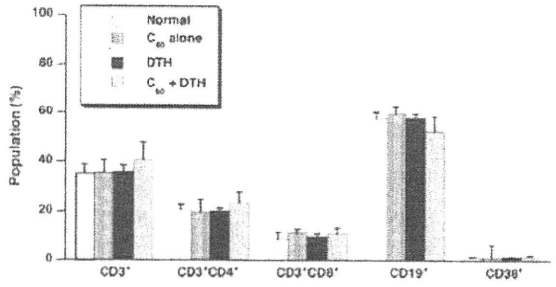

Fig. 6. Populations of splenic lymphocytes in normal, nano-C_{60} alone, DTH, and nano-C_{60}-DTH-groups. Phenotypes were analyzed by flow cytometry. DTH, delayed-type hypersensitivity; PBS, phosphate-buffered saline; C_{60}, nano-C_{60}.

mice through the generation of oxidative stress, and in this study, we investigated the effect of nano-C_{60} in a mouse model. Contrary to our expectation, footpad swelling in DTH mice was significantly suppressed by nano-C_{60} treatment.

After antigen presentation by antigen-presenting cells (APC), undifferentiated helper T cells (naive T cells) differentiate into effector T cells, which can be classified into two different types, Th1 and Th2, based on the kinds of cytokine they produce. The Th1 cytokines promote cellular immunity by activating macrophages, cytotoxic $CD8^+$ T lymphocytes, etc., while the Th2 cytokines enhance humoral immunity, including activation and class switching of antibody-producing B cells. The direction of naive T cell differentiation is determined by the kind of antigen and immunocyte with which the T cell interacts. An imbalance of cytokines produced by helper T cells is believed to play an important role in the development of allergy and autoimmune diseases (Charlton and Lafferty, 1995). It is generally accepted that Th1 cells play a pathogenic role in the development of DTH. IFN-γ, which is a representative Th1 cytokine produced by antigen-specific $CD4^+$ T cells, promotes DTH responses by enhancing Th1 cell development. Development of DTH in mice immunized with mBSA is therefore associated with

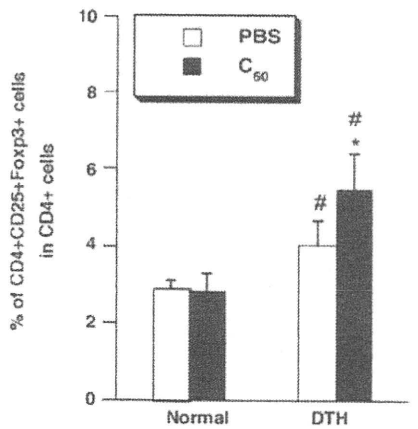

Fig. 7. Up-regulation of regulatory T cells in DTH mice treated with nano-C_{60}. The percentage of $CD4^+CD25^+Foxp3^+$ was analyzed by flow cytometry. Each value represents the mean ± S.E. ($n = 5$). PBS, phosphate-buffered saline; C_{60}, nano-C_{60}. *Statistically significant difference ($P < 0.05$) compared to the normal control group. #Statistically significant difference ($P < 0.05$) compared to the DTH-disease control group.

elevation of pro-inflammatory cytokines such as IL-6, IL-17 and TNF-α. Interestingly, the elevations of pro-inflammatory cytokines, except for TNF-α, in our DTH mice model were significantly suppressed by nano-C_{60} treatment, in accordance with the observed inhibitory effect of nano-C_{60} on the pathological paw swelling. However, the elevated production of TNF-α in DTH mice was further increased by nano-C_{60} treatment. TNF-α plays an important role in the elicitation phase of inflammation, so this finding seems in conflict with the observed attenuation of footpad swelling. Further study is needed to understand the mechanisms involved. As regards Th1/Th2 balance, the increased production of IFN-γ in DTH mice was not suppressed by nano-C_{60} treatment, but that of IL-4 was suppressed, resulting in a switch of the balance toward Th1-dominant immunity. Though IFN-γ plays an important role in the development of DTH, as mentioned above, the clinical severity and pathology of DTH were reported to be exacerbated in IFN-γ knockout mice (Jones et al., 1997). This phenomenon was found not only in DTH, but also in other Th1-related autoimmune diseases, including collagen-induced arthritis (CIA) and experimental autoimmune encephalomyelitis (EAE) (Caspi et al., 1994; Ferber et al., 1996). Namely, though IFN-γ is indispensable for development of DTH, it also appears to have a protective effect against these diseases. This seems paradoxical from the viewpoint of the Th1 paradigm of DTH. However, the apparent paradox could be resolved by considering the role of Th17 cells. These cells are a newly identified helper T cell subset, distinct from Th1 and Th2 cells (Harrington et al., 2006); they express CD4 and orphan nuclear receptor RORγt, and produce IL-17. It was reported that DTH responses induced by mBSA were impaired in IL-17-deficient mice; IL-17 was required for allergen-specific T cell activation in the sensitization phase during DTH (Afzali et al., 2007). IL-17 enhances the production of pro-inflammatory cytokines, including IL-1, IL-6 and TNF-α, and chemokines, and acts together with these cytokines, though it has no direct pathological effect (Furuzawa-Carballeda et al., 2007). Nano-C_{60} treatment markedly suppressed the production of IL-17 in DTH mice (Fig. 3), and this finding was confirmed *in vitro* (Fig. 5), suggesting that nano-C_{60} may act directly on IL-17 synthesis in Th17 cells.

Treg cells also constitute a distinct subset that ameliorates immune pathology through suppression of pathogenic T cells (Tanaka and Sakaguchi, 2005). In contrast with the aggravating function of Th17 cells on autoimmune diseases, Treg cells have a critical function in the regulation of autoimmune diseases, including DTH (Fontenot et al., 2003; Sakaguchi, 2004; Sato et al., 2006). Treg cells express CD4, IL-2 receptor α chain (CD25), and transcriptional factor Foxp3 (Vicki, 2003). The suppressive action of Treg is due to release of inhibitory cytokines and cellular interaction. The percentage of Treg in $CD4^+$ T cells was significantly increased by nano-C_{60} treatment in DTH disease control mice (Fig. 7). Both Th17 cells and Treg cells are differentiated from naive $CD4^+$ T cells, and the pathways are mutually exclusive. Naive $CD4^+$ T cells will differentiate to Th17 cells in the presence of TGF-β and IL-6, and to Treg cells in the presence of TGF-β and absence of IL-6 (Bettelli et al., 2006; Mangan et al., 2006). In addition, IL-6 is an inflammatory cytokine that is involved in the development of DTH. Our results indicate that nano-C_{60} treatment significantly suppressed the elevation of IL-6 in DTH disease-control mice (Fig. 3). These results would suggest that a decrease of IL-6 production by splenic lymphocytes plays a significant role in the inhibitory effect of nano-C_{60} on DTH. Further study to examine the mechanisms in detail is under way.

Conflict of interest

None.

Acknowledgments

This research was supported in part by a Grant-in-Aid for the private University Science Research Upgrade Promotion Business Academic Frontier Project.

References

Afzali, B., Lombardi, G., Lechler, R.I., Lord, G.M., 2007. The role of T helper 17 (Th17) and regulatory T cells (Treg) in human organ transplantation and autoimmune disease. Clin. Exp. Immunol. 148 (1), 32–46.

Bettelli, E., Carrier, Y., Gao, W., Korn, T., Strom, T.B., Oukka, M., Weiner, H.L., Kuchroo, V.K., 2006. Reciprocal developmental pathways for the generation of pathogenic effector Th17 and regulatory T cells. Nature 441, 235–238.

Black, C.A., 1999. Delayed type hypersensitivity: current theories with an historic perspective. Dermatol. Online J. 5, 1–7.

Bosi, S., Da Ros, T., Spalluto, G., Prato, M., 2003. Fullerene derivatives: an attractive tool for biological applications. Eur. J. Med. Chem. 38, 913–923.

Briviba, K., Klotz, L.O., Sies, H., 1997. Toxic and signaling effects of photochemically or chemically generated singlet oxygen in biological systems. Biol. Chem. Hoppe-Seyler 378, 1259–1265.

Brown, D.M., Wilson, M.R., MacNee, W., Stone, V., Donaldson, K., 2001. Size-dependent proinflammatory effects of ultrafine polystyrene particles: a role for surface area and oxidative stress in the enhanced activity of ultrafines. Toxicol. Appl. Pharmacol. 175, 191–199.

Caspi, R.R., Chan, C.C., Grubbs, B.G., Silver, P.B., Wiggert, B., Parsa, C.F., Bahmanyar, S., Billiau, A., Heremans, H., 1994. Endogenous systemic IFN-gamma has a protective role against ocular autoimmunity in mice. J. Immunol. 152, 890–899.

Charlton, B., Lafferty, K.J., 1995. The Th1/Th2 balance in autoimmunity. Curr. Opin. Immunol. 7, 793–798.

Da Ros, T., Prato, M., 1999. Medicinal chemistry with fullerenes and fullerene derivatives. Chem. Commun., 663–669.

Deguchi, S., Alargova, R.G., Tsujii, K., 2001. Stable dispersions of fullerenes, C_{60} and C_{70} in water, preparation and characterization. Langmuir 17 (19), 6013–6017.

Diaz-Sanchez, D., 1997. The role of diesel exhaust particles and their associated polyaromatic hydrocarbons in the induction of allergic airway disease. Allergy 52, 52–58.

Diaz-Sanchez, D., Tsien, A., Fleming, J., Saxon, A., 1997. Combined diesel exhaust particulate and ragweed allergen challenge markedly enhances human in vivo nasal ragweed-specific IgE and skews cytokine production to a T helper cell 2-type pattern. J. Immunol. 158, 2406–2413.

Emerich, D.F., Thanos, C.G., 2003. Nanotechnology and medicine. Expert Opin. Biol. Ther. 3, 655–663.

Ferber, I.A., Brocke, S., Taylor-Edwards, C., Ridgway, W., Dinisco, C., Steinman, L., Dalton, D., Fathman, C.G., 1996. Mice with a disrupted IFN-gamma gene are susceptible to the induction of experimental autoimmune encephalomyelitis (EAE). J. Immunol. 156, 5–7.

Fontenot, J.D., Gavin, M.A., Rudensky, A.Y., 2003. Foxp3 programs the development and function of CD4+CD25+ regulatory T cells. Nat. Immunol. 4, 330–336.

Fujimaki, H., Saneyoshi, K., Shiraishi, F., Imai, T., Endo, T., 1997. Inhalation of diesel exhaust enhances antigen-specific IgE antibody production in mice. Toxicology 116, 227–233.

Furuzawa-Carballeda, J., Vargas-Rojas, M.I., Cabral, A.R., 2007. Autoimmune inflammation from the Th17 perspective. Autoimmunity Rev. 6, 69–75.

Guldi, D.M., Prato, M., 2000. Excited-state properties of C_{60} fullerene derivatives. Accounts Chem. Res. 33 (10), 695–703.

Haley, K.J., Drazen, J.M., 1998. Inflammation and airway function in asthma: what you see is not necessarily what you get. Am. J. Resp. Crit. Care Med. 157, 1–3.

Harrington, L.E., Mangan, P.R., Weaver, C.T., 2006. Expanding the effector CD4 T-cell repertoire: the Th17 lineage. Curr. Opin. Immunol. 18, 349–356.

Ichinose, T., Furuyama, A., Sagai, M., 1995. Biological effects of diesel exhaust particles (DEP). II. Acute toxicity of DEP introduced into lung by intratracheal instillation. Toxicology 99, 153–167.

Jones, L.S., Rizzo, L.V., Agarwal, R.K., Tarrant, T.K., Chan, C.C., Wiggert, B., Caspi, R.R., 1997. IFN-gamma-deficient mice develop experimental autoimmune uveitis in the context of a deviant effector response. J. Immunol. 158, 5997–6005.

Kariyone, A., Tamura, T., Kano, H., Iwakura, Y., Takeda, K., Akira, S., Takatsu, K., Immunogenicity of peptide-25 of Ag85B in Th1 development: role of IFN-gamma. Int. Immunol. 15, 1183–1194.

Kobayashi, K., Kanedam, K., Kasamam, T., 2001. Immunopathogenesis of delayed-type hypersensitivity. Microsc. Res. Tech. 53, 241–245.

Kroto, H.W., Heath, J.R., Brein, S.O., Curl, R.F., Smalley, R.R., 1985. C_{60}: Buckminsterfullerene. Nature 318, 162–163.

Mangan, P.R., Harrington, L.E., O'Quinn, D.B., Helms, W.S., Bullard, D.C., Elson, C.O., Hatton, R.D., Wahl, S.M., Schoeb, T.R., Weaver, C.T., 2006. Transforming growth factor-beta induces development of the Th17 lineage. Nature 441, 231–234.

Moghimi, S.M., Hunter, A.C., Murray, J.C., 2005. Nanomedicine: current status and future prospects. J. Fed. Am. Soc. Exp. Biol. 19, 311–330.

Nakae, S., Komiyama, Y., Nambu, A., Sudo, K., Iwase, M., Homma, I., Sekikawa, K., Asano, M., Iwakura, Y., 2002. Antigen-specific T cell sensitization is impaired in IL-17-deficient mice, causing suppression of allergic cellular and humoral responses. Immunity 17, 375–387.

Oberdörster, E., 2004. Manufactured nanomaterials (fullerenes, C_{60}) induce oxidative stress in the brain of juvenile largemouth bass. Environ. Health. Persp. 112, 1058–1062.

Oberdörster, G., Oberdörster, E., Oberdörster, J., 2005. Nanotoxicology: an emerging discipline evolving from studies of ultrafine particles. Environ. Health. Persp. 113, 823–839.

Osawa, E., 1970. Fullerene. Kagaku. 25, 854–863.

Sakaguchi, S., 2004. Naturally arising CD4+ regulatory t cells for immunologic self-tolerance and negative control of immune responses. Ann. Rev. Immunol. 22, 531–562.

Sato, K., Suematsu, A., Okamoto, K., Yamaguchi, A., Morishita, Y., Kadono, Y., Tanaka, S., Kodama, T., Akira, S., Iwakura, Y., Cua, D.J., Takayanagi, H., 2006. Th17 functions as an osteoclastogenic helper T cell subset that links T cell activation and bone destruction. J. Exp. Med. 203, 2673–2682.

Satoh, M., Takayanagi, I., 2006. Pharmacological studies on fullerene (C_{60}), a novel carbon allotrope, and its derivatives. J. Pharmacol. Sci. 100, 513–518.

Sayes, C.M., Gobin, A.M., Ausman, K.D., Mendez, J., West, J.L., Colvin, V.L., 2005. Nano-C_{60} cytotoxicity is due to lipid peroxidation. Biomaterials 26, 7587–7595.

Särnstrand, B., Jansson, A.H., Matuseviciene, G., Scheynius, A., Pierrou, S., Bergstrand, H., 1999. N,N′-Diacetyl-L-cystine—the disulfide dimer of N-acetylcysteine is a potent modulator of contact sensitivity/delayed type hypersensitivity reactions in rodents. J. Pharmacol. Exp. Ther. 288, 1174–1184.

Tagmatarchis, N., Shinohara, H., 2001. Fullerenes in medicinal chemistry and their biological applications. Mini Rev. Med. Chem. 1, 339–348.

Takano, H., Yoshikawa, T., Ichinose, T., Miyabara, Y., Imaoka, K., Sagai, M., 1997. Diesel exhaust particles enhance antigen-induced airway inflammation and local cytokine expression in mice. Am. J. Resp. Crit. Care Med. 156, 36–42.

Tanaka, S., Sakaguchi, S., 2005. Regulatory T cell and autoimmune diseases. Jpn. J. Immunol. 28, 291–299.

Vicki, L.C., 2003. Characterizing the potential risks posed by engineered nanoparticles. Nat. Biotechnol. 21, 1166–1170.

Yoshimoto, T., Wang, C.R., Yoneto, T., Matsuzawa, A., Cruikshank, W.W., Nariuchi, H., 2000. Role of IL-16 in delayed-type hypersensitivity reaction. Blood 95, 2869–2874.

Bioorganic & Medicinal Chemistry Letters 18 (2008) 3582–3584

Contents lists available at ScienceDirect

Bioorganic & Medicinal Chemistry Letters

journal homepage: www.elsevier.com/locate/bmcl

Synthesis of new UV-B light absorbents: (Acetylphenyl)glycosides with antioxidant activities

Takashi Otani [a], Tetsu Tsubogo [a], Naoki Furukawa [a], Takao Saito [a,*], Katsumi Uchida [b], Kanako Iwama [b], Yuki Kanai [b], Hirofumi Yajima [b,*]

[a] Department of Chemistry, Faculty of Science, Tokyo University of Science, Kagurazaka, Shinjuku-ku, Tokyo 162-8601, Japan
[b] Department of Applied Chemistry, Faculty of Science, Tokyo University of Science, Kagurazaka, Shinjuku-ku, Tokyo 162-8601, Japan

ARTICLE INFO

Article history:
Received 3 January 2008
Revised 17 April 2008
Accepted 1 May 2008
Available online 6 May 2008

Keywords:
UV-B light absorbents
Antioxidant activities
Synthesis
Glycosides

ABSTRACT

m-Acetylphenyl-β-D-glucopyranosides and *m*-acetylphenyl-α/β-D-mannopyranosides were synthesized by the Koenigs–Knorr, Mitsunobu, and Helferich reactions as key glycosylation reactions, respectively. Their spectroscopic properties and antioxidative activities were characterized as potential ultraviolet B-ray absorbents.

Ultraviolet (UV) light in the sunlight is an environmental human carcinogen. UV light in sunlight is divided into three regions, viz. UV-A (320–400 nm), UV-B (280–320 nm), and UV-C (200–280 nm). The stratospheric ozone layer effectively blocks UV-C light from reaching the earth's surface. Both UV-A and UV-B light reach the earth's surface in sufficient amounts to give rise to serious biological consequences to the skin and eyes. Although UV-A light is the predominant component of terrestrial UV radiation and believed to be rather weak in the carcinogenesis, excessive exposure to UV-A light causes aging and wrinkling of the skin.[1] On the other hand, UV-B light is known to be absorbed into the skin, producing erythema, burns, and eventually skin cancer as a consequence of DNA damage.

The eye lenses of diurnal primates contain glucosides that act as UV filters. Glucosides **1–4** were isolated and their structures identified.[2–5] (3-Acetyl-2-aminophenyl)-β-D-glucopyranoside (**3**: AAP-β-D-Glu) is known to be the precursor of yellow pigments, whose intensity increases with age.[4,6] Therefore, AAP-β-Glu (**3**) containing an acetylaminophenyl group as an aglycon is expected to serve as a UV-A absorbent in sunscreen for cosmetics. It should be noted that an aromatic amino group of a liberated aglycon has been suspected of being venomous. Satoh et al.[6] showed that AAP-β-Glu (**3**) would be involved in photodynamic processes at work in the aging human lens. Moreover, they suggested that photooxidation proceeded with an increase in accumulation of active oxygen generated through the aglycon, and that the active oxygen formed is diminished by the in situ presence of the glycon of the glucoside, acting as an antiphotooxidant. With regard to the antioxidant functions of sugars, West et al. presented the radical scavenger processes for hydroxyl radical (·OH).[7] In the sugar species, it has been reported that the antioxidant activity increases in the order glucose < mannose ≤ fructose.[8]

The objective of this study was to develop a new UV-B light absorbent by modification of the glycoside **3**. In taking account of the foregoing context, including the order of the sugar species for antioxidant activity, we synthesized *m*-acetylphenyl-β-D-mannopyranosides (**5**: AP-β-Man) composed of an acetylphenyl group as an aglycon and mannose as a glycon. The removal of the electron-releasing amino group (–NH_2) from 2-amino-3-hydroxyacetophenone (AHA) of the aglycon in AAP-β-Glu (**3**) is predicted to give rise to a blue shift of the characteristic absorption band from the UV-A range to the UV-B range. For comparison, *m*-acetylphenyl-β-D-glucopyranosides (**6**: AP-β-Glu) and *m*-acetylphenyl-α-D-mannopyranoside (**7**: AP-α-Man) were also synthesized. The spectroscopic properties such as the UV–vis absorption and fluorescence spectra were probed for the glycosides **5–7**. Moreover, their antioxidant activities were evaluated by monitoring the increments of the absorbances at 550 nm responsible for the photogeneration of superoxide anion radical (O_2^{-}) using the cytochrome-*c* reduction assay[9] (see the Supplementary Data for details). The effects of the sugar species and anomer on the physicochemical properties of the glycosides will be discussed below.

* Corresponding authors. Tel.: +81 3 52288254; fax: +81 3 52614631 (T. Saito).
E-mail addresses: tsaito@ch.kagu.tus.ac.jp, tsaito@rs.kagu.tus.ac.jp (T. Saito).

0960-894X/$ - see front matter © 2008 Elsevier Ltd. All rights reserved.
doi:10.1016/j.bmcl.2008.05.006

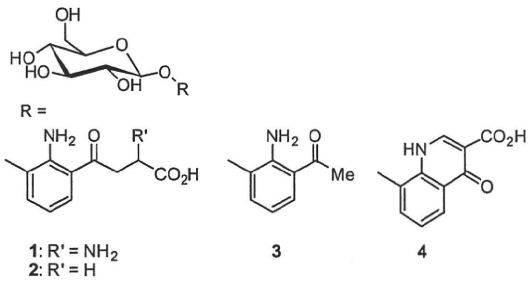

The AP-β-Man **5** was synthesized by the Mitsunobu reaction[10] as a key reaction by a two-step procedure without resorting to chromatographic purification (Scheme 1).[11] First, D-mannose (**8**) was converted to crystalline 2,3;4,6-di-*O*-cyclohexylidene-α-D-mannopyranose (**9**) by reaction with 1-ethoxycyclohexene. The protected mannose **9** was glycosylated with *m*-hydroxyacetophenone (**10**) under the Mitsunobu conditions to produce mannopyranoside **11**, which was hydrolyzed with acetic acid to give AP-β-Man (**5**) in 56% yield.[12]

The glucosides **6** were prepared by Koenigs–Knorr glycosylation (Scheme 2).[13] D-Glucose (**12**) was converted to 2,3,4,6-tetra-*O*-acetyl-α-D-glucopyranosyl bromide (**13**) in high yield, which was then glycosylated with *m*-hydroxyacetophenone (**10**) by the Koenigs–Knorr glycosylation to produce β-glycoside **14** (29%). Deprotection of the acetyl groups of **14** with sodium methoxide gave AP-β-Glu (**6**) (60%).[14]

The α-mannopyranoside **7** was prepared by the Helferich reaction[15] as a key reaction (Scheme 3).[16] Treatment of D-mannose (**8**) with acetic anhydride in the presence of pyridine gave the pentaacetate **15** in high yield.[17] The pentaacetate **15** was reacted with **10** upon heating in the presence of $ZnCl_2$ to give α-glycosylated mannose **16** in 41% yield. Deprotection of **16** under basic conditions produced AP-α-Man (**7**) in 30% yield.[18]

Figure 1 shows the UV–vis absorption spectra of HA (**10**), AP-β-Man (**5**), AP-β-Glu (**6**), and AP-α-Man (**7**), which were measured with a JASCO V-570 spectrophotometer. All the samples including the aglycon HA (**10**) gave absorption spectra with three peaks at around 210, 250, and 300 nm in the UV-B region. Compared with the spectral feature of HA, the glycosides **5–7** exhibited blue shifts for each of the peaks, accompanied by a slight hypochromic effect for the band near 300 nm and bathochromic effects for the bands near 210 and 250 nm. Each of the glycosides **5–7** has a moderate UV-B absorbance with molar extinction coefficients $\varepsilon_{300} \approx 2000\ M^{-1}\ cm^{-1}$ at 300 nm, regardless of the sugar species and anomer. The ε_{300} values of all the samples are summarized

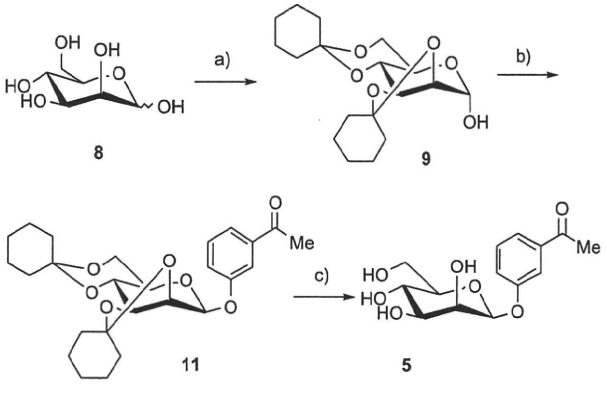

Scheme 1. Reagents and conditions: (a) 1-ethoxycyclohexene, *p*-TsOH (cat.), DMF 44%; (b) *m*-hydroxyacetophenone (**10**), DEAD, TPP, toluene; (c) AcOH, H_2O 56% in two steps.

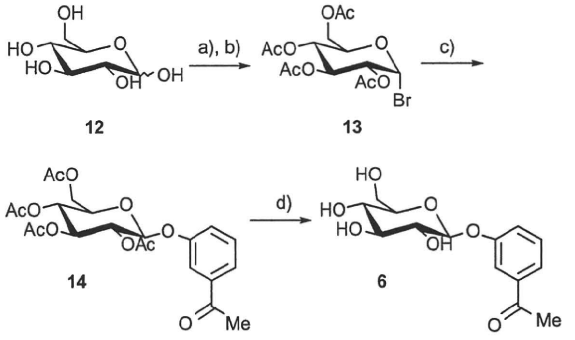

Scheme 2. Reagents and conditions: (a) Ac_2O, cat. $HClO_4$; (b) P, Br_2, H_2O; (c) **10**, Ag_2O, $CaSO_4$, pyridine, I_2 29%; (d) NaOMe, MeOH, H_2O, 60%.

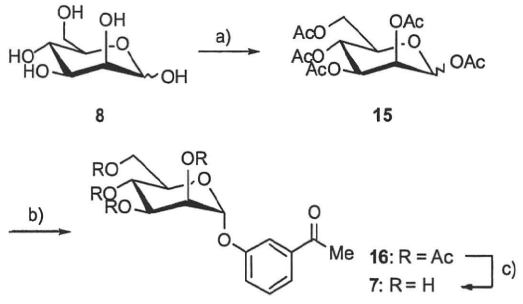

Scheme 3. Reagents and conditions: (a) Ac_2O, pyridine; (b) **10**, $ZnCl_2$, AcOH/Ac_2O 150 °C 41%; (c) MeONa, MeOH 30%.

in Table 1, including the antioxidation efficiencies (AO). It should be noted that the ε_{360} value of the AAP-β-Glu (**3**) at 360 nm in the UV-A region is ca. 3400 $M^{-1}\ cm^{-1}$.[4] Typical excitation (Ex) and fluorescence spectra (Em) of AP-β-Man (**5**) in aqueous solution are shown in Figure 2, where the emission wavelength for the former and excitation wavelength for the latter were $\lambda_{em} = 400$ nm and $\lambda_{ex} = 320$ nm, respectively. Likewise, the other glycosides, AP-β-Glu (**6**) and AP-α-Man (**7**) besides HA (**10**) exhibited similar Ex and Em spectra to those of AP-β-Man (**5**). The Ex spectra showed peaks at around 275 and 325 nm, whereas the Em spectra showed a peak at around 400 nm, regardless of the sugar species and anomer.

Table 1 shows the AO values estimated by the following formula (Eq. 1) from the cytochrome-*c* reduction assay[9]:

$$AO(\%) = \left(1 - \frac{\Delta A_{550}}{\Delta A^{0}_{550}}\right) \times 100, \quad (1)$$

where ΔA^{0}_{550} and ΔA_{550} refer to the increments in the absorbances at 550 nm over the reaction time of 1 h for aglycon HA (**10**) and each of the glycosides **5–7**. All of the glycosides **5–7** show antioxidant activities, in particular, the AO value of AP-β-Man (**5**) is the largest.

It should be noted that the synthesized glycoside **5** has also efficient antioxidant activity for singlet oxygen generated in the photo reaction (based on the squaleneperoxide assay, see the Supplementary Data for details).

In conclusion, new UV-B absorbent glycosides **5–7** with efficient antioxidant activity were synthesized. The results show that AP-β-Man (**5**) is expected to serve as a potential UV-B absorbent in sunscreen for cosmetics.[19]

Supplementary data

Supplementary data associated with this article can be found, in the online version, at doi:10.1016/j.bmcl.2008.05.006.

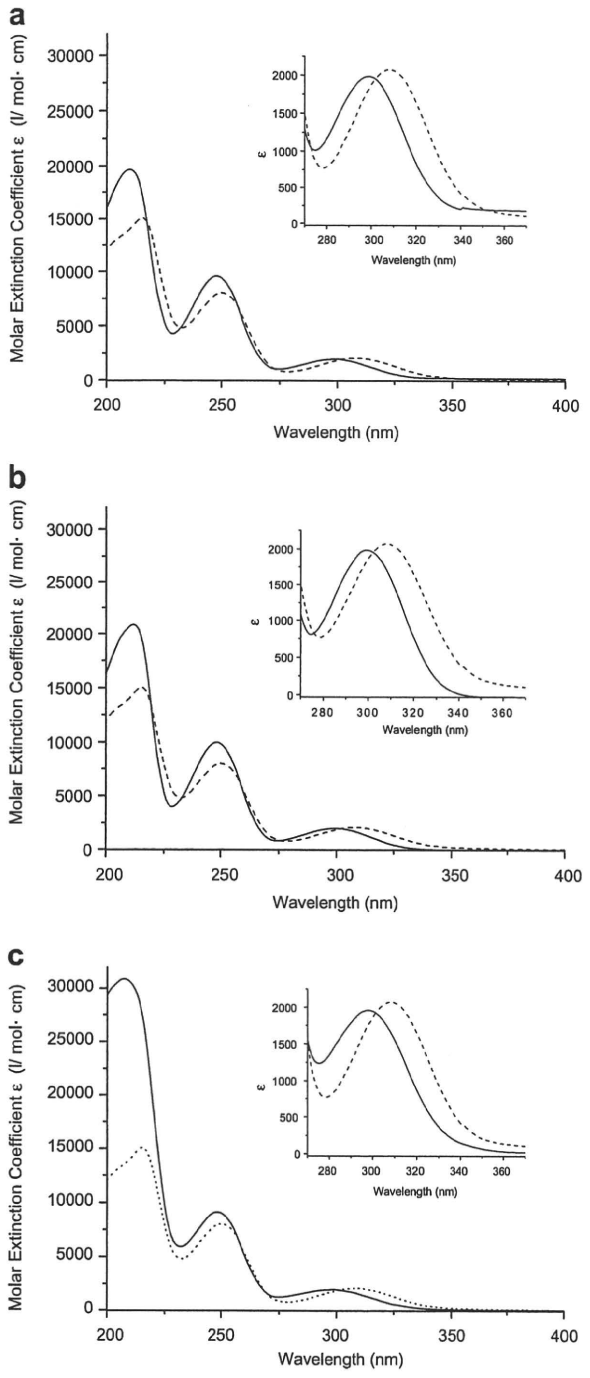

Figure 1. Absorption spectra of glycosides (**5**, a; **6**, b; **7**, c) in solid line and aglycon HA (**10**) in a dashed line. Insets: magnification of UV-B region of spectra.

Table 1
Molar extinction coefficients ε_{300} at 300 nm and degree of antioxidant activity (AO) for HA (**10**) and the glycosides **5–7**

Compound	ε_{300} (M^{-1} cm^{-1})	AO (%)
HA (**10**)	1870	0.0
AP-β-Man (**5**)	1946	71.5
AP-β-Glu (**6**)	1982	51.7
AP-α-Man (**7**)	1976	66.9

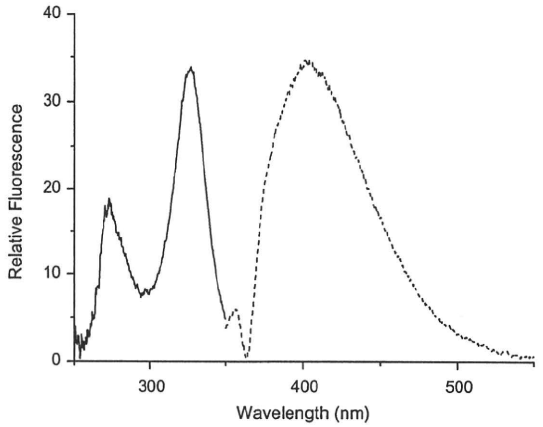

Figure 2. Excitation (solid line) and emission (dashed line) spectra of AP-β-Man (**5**).

References and notes

1. Matsumura, Y.; Ananthaswamy, H. N. *Toxicol. Appl. Pharmacol.* **2004**, *195*, 298.
2. van Heyningen, R. *Nature* **1971**, *230*, 393.
3. (a) Inoue, A.; Satoh, K. *Bioorg. Med. Chem. Lett.* **1994**, *4*, 2303; (b) Truscott, R. J. W.; Wood, A. M.; Carver, J. A.; Sheil, M. M.; Stutchbury, G. M.; Zhu, J.; Kilby, G. W. *FEBS Lett.* **1994**, *348*, 173; (c) Chenault, H. K.; Yang, Jie; Taber, D. F. *Tetrahedron* **2000**, *56*, 3673.
4. (a) Inoue, A.; Satoh, K. *Bioorg. Med. Chem. Lett.* **1993**, *3*, 345; (b) Das, S. K.; Saha, U. K. *Bioorg. Med. Chem. Lett.* **1994**, *4*, 1219.
5. Shirao, E.; Ando, K.; Inoue, A.; Shirao, Y.; Balasubramanian, D. *Exp. Eye Res.* **2001**, *73*, 421.
6. Inoue, A.; Sasaki, D.; Satoh, K. *Exp. Eye Res.* **2004**, *79*, 833.
7. West, P. R.; Schnarr, G. W.; Sitwell, L. *Tetrahedron Lett.* **1977**, *18*, 3869.
8. Grankvist, K. *Biochem. J.* **1981**, *200*, 685.
9. Rajendran, M.; Inbaraj, J. J.; Gandhidasan, R.; Murugesan, R. *J. Photochem. Photobiol. A* **2006**, *182*, 67.
10. Mitsunobu, O. *Synthesis* **1981**, 1.
11. (a) Garegg, P. J.; Iversen, T. *Carbohydr. Res.* **1979**, *70*, C13; (b) Garegg, P. J.; Iversen, T.; Norberg, T. *Carbohydr. Res.* **1979**, *73*, 313.
12. **5**: colorless solid, mp 64.4–65.0 °C; ^{1}H NMR (500 MHz, D_2O, δ): 7.72 (d, J = 7.8 Hz, 1H, 4′-H), 7.62 (s, 1H, 2′-H), 7.51 (t, J = 8.0 Hz, 1H, 5′-H), 7.37 (dd, J = 2.6, 8.2 Hz, 1H, 6′-H), 5.41 (s, 1H, 1-H), 4.23 (d, J = 3.3 Hz, 1H, 2-H), 3.92 (dd, J = 2.2, 12.4 Hz, 1H, 6-H), 3.80–3.76 (m, 1H, 3-H), 3.75 (d, J = 6.6 Hz, 1H, 6-H), 3.69 (t, J = 9.8 Hz, 1H, 4-H), 3.62–3.57 (m, 1H, 5-H), 2.65 (s, 3H, CH_3); ^{13}C NMR (150 MHz, D_2O, δ): 203.1 (C=O), 156.3 (C), 137.7 (C), 130.1 (CH), 123.2 (CH), 121.8 (CH), 115.3 (CH), 97.4 (CH), 76.4 (CH), 72.6 (CH), 70.4 (CH), 66.6 (CH), 60.1 (CH_2), 26.2 (CH_3); HRMS-FAB (m/z): $[M+H]^+$ Calcd for $C_{14}H_{19}O_7$, 299.1131; found 299.1129.
13. Koenig, W.; Knorr, E. *Ber* **1901**, *34*, 957.
14. **6**: Colorless solid, mp 172.0–173.1 °C; ^{1}H NMR (600 MHz, D_2O, δ): 7.74 (d, J = 7.7 Hz, 1H, 4′-H), 7.66 (s, 1H, 2′-H), 7.53 (t, J = 8.0 Hz, 1H, 5′-H), 7.40 (dd, J = 2.4, 9.1 Hz, 1H, 6′-H), 5.18 (d, J = 7.1 Hz, 1H, 1-H), 3.94 (dd, J = 1.7, 12.4 Hz, 1H, 6-H), 3.74 (dd, J = 6.1, 12.4 Hz, 1H, 6-H), 3.62–3.56 (m, 1H, 5-H), 3.56–3.48 (m, 2H, 2-H and 3-H), 3.50 (t, J = 9.2 Hz, 1H, 4-H), 2.66 (s, 3H, CH_3); ^{13}C NMR (150 MHz, D_2O, δ): 206.8 (C=O), 159.4 (C), 140.8 (C), 133.0 (CH), 126.3 (CH), 124.9 (CH), 118.5 (CH), 102.9 (CH), 79.0 (CH), 78.3 (CH), 75.6 (CH), 72.2 (CH), 63.3 (CH_2), 29.1 (CH_3); HRMS-FAB (m/z): $[M+H]^+$ Calcd for $C_{14}H_{19}O_7$, 299.1131; found 299.1130.
15. Helferich, B.; Schmitz-Hillebrecht, E. *Ber* **1933**, *378*, 66.
16. (a) Conchie, J.; Levvy, G. A. *Methods Carbohydr. Chem.* **1963**, 345; (b) Vervoort, A.; De Bruyne, C. K. *Carbohydr. Res.* **1970**, *12*, 277.
17. Levene, P. A. *J. Biol. Chem.* **1924**, *59*, 141.
18. **7**: colorless solid, mp 161.2–162.2 °C; ^{1}H NMR (600 MHz, D_2O, δ): 7.72 (d, J = 3.3 Hz, 1H, 4′-H), 7.69 (s, 1H, 2′-H), 7.51 (dd, J = 7.8, 8.2 Hz, 1H, 5′-H), 7.43 (dd, J = 1.7, 8.2 Hz, 1H, 6′-H), 5.67 (d, J = 1.7 Hz, 1H, 1-H), 4.20 (dd, J = 1.7, 3.7 Hz, 1H, 2-H), 4.06 (dd, J = 3.4, 9.2 Hz, 1H, 3-H), 3.82–3.68 (m, 4H, 4-H, 5-H, and 6-H), 2.65 (s, 3H, CH_3); ^{13}C NMR (150 MHz, D_2O, δ): 203.3 (C=O), 155.5 (C), 137.9 (C), 130.1 (CH), 123.2 (CH), 122.5 (CH), 116.4 (CH), 98.1 (CH), 73.4 (CH), 70.3 (CH), 69.8 (CH), 66.5 (CH), 60.6 (CH_2), 26.3 (CH_3); HRMS-ESI (m/z): $[M+Na]^+$ Calcd for $C_{14}H_{18}NaO_7$, 321.0945; found 321.0934.
19. Satoh, K.; Yajima, H.; Saito, T.; Uchida, K.; Otani, T.; Iwama, K.; Tsubogo, T. (Tokyo University of Science, Japan). Jpn. Kokai Tokkyo Koho JP 2007230879 A 20070913, 2007.

Exp. Anim. 59(2), 255–260, 2010

—Note—

Fetal Sex Determination of Macaque Monkeys by a Nested PCR Using Maternal Plasma

Fusako MITSUNAGA[1,2], Miyuki UEIWA[1], Yoshirou KAMANAKA[1], Mayumi MORIMOTO[1], and Shin NAKAMURA[1]

[1]*Department of Cellular and Molecular Biology, Primate Research Institute, Kyoto University, 41–2 Kanrin, Inuyama, Aichi 484-8506 and* [2]*NPO Primate Agora, Kurisu, Inuyama, Aichi 484-0002, Japan*

Abstract: Non-invasive fetal sex determination is required for biomedical studies, in which some sexual difference would be expected in fetal events, in order to make a choice of male or female fetus. To detect male fetal DNA of the sex-determining region Y gene (*SRY*) in maternal macaque plasma, nested real-time PCR using the SYBR Green system was developed. In all cases of pregnant macaques with male fetuses, a nested PCR product of SRY was amplified from the mother's plasma, while no amplicon was detected in any case of pregnancy with a female fetus. Interestingly, fetal SRY DNA appeared to be cleared rapidly from the maternal blood after parturition. The current method is sensitive and can be performed with a regular PCR machine.

Key words: fetal DNA, maternal blood, *SRY*

Non-human primates, especially macaques, are invaluable experimental animals in biomedical studies because of the close relationship between their biological nature and that of humans [11]. It is well known that their reproductive characteristics, placental structure and developmental events are very similar to those of humans [6]. This is why macaques are widely used in studies of fetal development, and the fetal influence of drugs/substances transferred through the placenta [9]. Prenatal determination of the fetal sex is required in these studies when sex differences in the fetal response to administered drugs or substances are anticipated. Detection of male fetal DNA (fDNA) in maternal blood has been developed as a non-invasive method for fetal sex determination [7] instead of amniocentesis. Since the amount of fDNA circulating in maternal blood is very low [8], a much more sensitive and accurate method is needed. Recently, real-time PCR with the TaqMan system was reported to detect male fDNA in the serum of pregnant macaques [5]. However, the TaqMan real-time PCR method requires a specific TaqMan probe and expensive real-time PCR apparatus.

In the present study, we established a nested PCR method to detect the fetal male DNA sequence of the sex determining region Y (*SRY*) gene in maternal plasma. This nested PCR method makes it possible to perform fetal sex determination not only with real-time PCR apparatus, but also with a regular PCR machine.

Animals: Pregnant rhesus macaques (*Macaca mulatta*, total number: 21, mean age: 10.8 ± 3.8 years) at the Primate Research Institute (PRI), Kyoto University, Japan were used in this study. The macaques were housed

(Received 2 September 2009 / Accepted 22 November 2009)

Address corresponding: S. Nakamura, Department of Molecular and Cellular Biology, Primate Research Institute, Kyoto University, 41–2 Kanrin, Inuyama, Aichi 484-8506, Japan

GATAAAGTGAAGCGACCCATGAACGCATTCATTGTGTGGTC
TCGCGATCAGAGGCGCAAGATGGCTCTAGAGAATCCCAAAA
TGCGAAACTCAGAGATCAGCAAGCAGCTGGGATACCAGTGG
AAAATGCTTACCGAAGCCGATAAATGGCCATTCTTCCAGGA
GGCACAGAAACTACAGGCCATGCATAGAGAGAAATACCCGA
ATTATAAGTATCGACCTCGTCGGAAGGCGAAGATGCTG

Fig. 1. *SRY* gene sequence of *Macaca mulatta*. Nt344 to 583 of the published *SRY* gene sequence (Genbank accession number AF284310) is shown. Sequences within boxes indicate the primer binding sites for the first PCR. Underlined sequences indicate the primer binding sites of the second PCR. The amplicon of the nested PCR is 75 bp.

in individual cages or in group cages and were fed monkey chow supplemented with fresh fruits and vegetables. Experiments and animal husbandry were performed in accordance with the PRI's institutional guide for the care and use of laboratory primates, which is based on the 'Guide for the Care and Use of Laboratory Animals' by the US National Research Council, 1996 [1]. All experimental procedures were approved by the institutional animal care and use committee.

Gestational days (GD) were estimated using the date of timed mating and were confirmed by changes in the plasma levels of estradiol and progesterone by ELISA (Neogen Corp., Lexington, KY, USA) in early gestation [3]. Fetal age was also confirmed by measuring the biparietal diameter with ultrasonography from 6 weeks of gestation until term [10].

Blood sample collection and DNA extraction: Peripheral blood (2 ml) was collected into heparin-containing syringes from pregnant rhesus macaques during gestation of 42 to 183 days. Plasma samples were obtained by centrifugation of the blood at 1,000 *g* for 15 min and stored at –80°C until use. DNA was extracted from 800 μl of plasma using a QIAmp DNA Blood Kit (Qiagen, Tokyo, Japan) according to the manufacturer's instructions. DNA was eluted into a final volume of 40 μl and used as a PCR template.

Nested PCR with real-time apparatus using SYBR Green: Real-time PCR using SYBR Green as a product-reporting system was performed using an ABI Prism 7700 Sequence Detector (Applied Biosystems, Foster City, CA, USA) under the conditions described previously [4]. In brief, PCR was carried out in a 10-μl reaction mixture containing 1 μl of DNA template, 5 μl of 2× SYBR Premix Ex Taq (Takara Bio Inc., Otsu, Japan), 0.2 μl of 50× ROX Reference Dye (Takara Bio Inc.), and 2 pmol each of forward and reverse primers. The thermal conditions were 95°C for 10 s and 30 cycles of (95°C for 5 s, 63°C for 30 s) with generation of a dissociation curve at the end of the assay to verify the amplification of the target gene. The standard curves from GAPDH amplicons of known concentration were used to calculate the quantity of target genes in samples [4]. Figure 1 shows the sequence of the rhesus *SRY* gene (Genbank accession# AF284310) and the binding sites of specific primer pairs (SRY-1 and SRY-3, forward and reverse, respectively). The outer primer pair (SRY-1-forward, SRY-1-reverse) in this study was designed to amplify the sequence of the *SRY* gene in the first PCR. The inner primer pair (SRY-3-forward, SRY-3-reverse), which was described previously [2], was used to amplify a 75-bp fragment inside the amplicon of the first PCR. The sequences of these primers were as follows:

SRY-1-forward:
5'-GATAAAGTGAAGCGACCCATG -3';
SRY-1-reverse:
5'-CATCTTCGCCTTCCGACGAGG -3';
SRY-3-forward:
5'-CGATCAGAGGCGCAAGATG -3';
SRY-3-reverse:
5'-TGGTATCCCAGCTGCTTGCT -3';
GAPDH-forward:
5'-CCATGGAGAAGGCTGGGG -3';

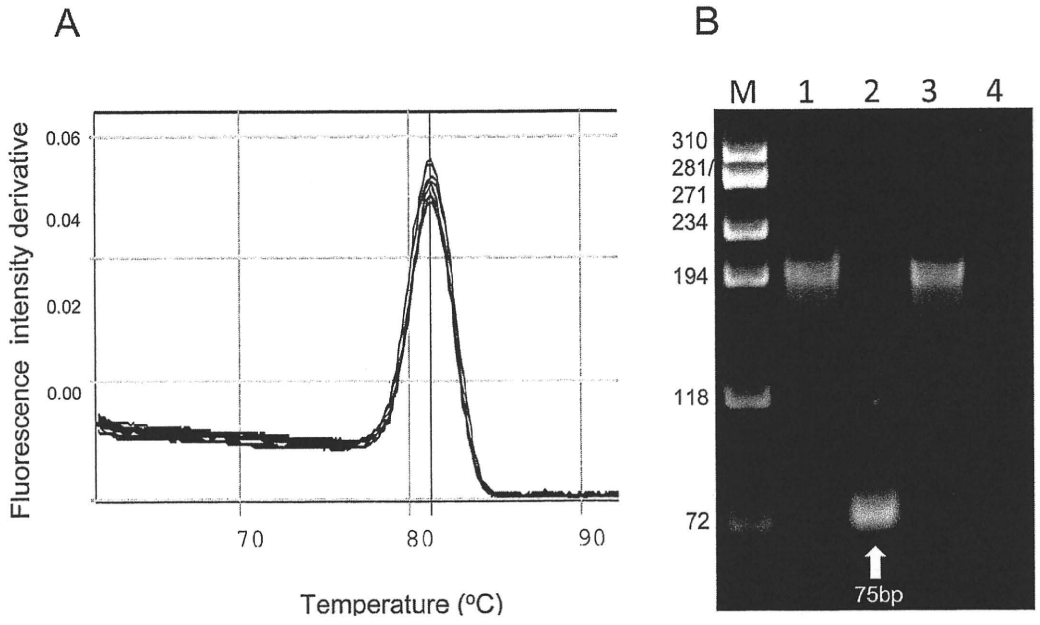

Fig. 2. Representative single PCR product obtained by nested PCR (SRY-3 primer set) of plasma DNA samples from pregnant macaques with male fetuses. A: Dissociation curves of SRY-3 fragment produced by real-time PCR. The temperature of its peak is 81.4°C. B: Polyacrylamide gel electrophoresis (PAGE) of GAPDH and SRY-3 amplicons. M: Marker (ϕX174/HaeIII). DNA samples from maternal plasma with male fetus (lanes 1 & 2) and with female fetus (lanes 3 & 4). PCR amplicon of GAPDH (lanes 1 & 3) and of SRY (lanes 2 & 4).

GAPDH-reverse:

5'-CAAAGTTGTCATGGATGACC -3'.

All PCRs were performed in triplicate for *SRY* sequences and in duplicate for the reference gene (*GAPDH*).

First PCR: The DNA samples extracted from plasma were used as the template in the first PCR, in which SRY DNA was amplified using the primer set of SRY-1. In the same PCR run, the number of copies of GAPDH fragments in each sample was assayed to estimate the DNA level in the template sample.

Second PCR: The first PCR plate was centrifuged briefly, and the PCR product of SRY-1 was collected. This first PCR product was diluted 1:100 and used as the template for the second PCR. The primer pair of SRY-3 was employed to amplify the inner sequence of the SRY-1 amplicon (Fig. 1).

Conventional nested PCR with regular PCR machine: Conventional nested PCR was performed under the same conditions as described above except that a regular PCR machine (Perkin-Elmer Inc., Waltham, MA, USA) was used. After the nested second PCR, the SRY-3 amplicon was subjected to polyacrylamide gel electrophoresis followed by staining with SYBR Green.

Sequence analysis of PCR product: PCR products were subjected to sequence analysis with an ABI Genetic Analyzer 310 (Applied Biosystems) to confirm their DNA sequences.

SRY DNA detection in pregnant macaques with male fetuses: After the first PCR using the SRY-1 primer set, all plasma DNA samples from pregnant macaques with male fetuses yielded an SRY DNA fragment by nested PCR using the SRY-3 primer set. The SRY-3 amplicon showed a symmetric dissociation curve with a peak of 81.4°C (Fig. 2A) and a single band of 75 bp in polyacrylamide gel electrophoresis (Fig. 2B). DNA sequence analysis of the nested PCR product revealed that the target sequence of SRY DNA was amplified using the nested PCR conditions (data not shown). However, plasma DNA samples from pregnant macaques with female fetuses yielded no SRY-3 amplicon by this nested PCR (Table 1). These findings indicate that the present nested PCR using primer sets SRY-1 for the first PCR

Table 1. Results of SRY-PCR and fetal sex

Gestation day[a)]	SRY[b)]	Fetal sex[c)]
42	+	male
52	+	male
91	+	male
115	+	male
130	+	male
135	+	male
137	+	male
150	+	male
156	+	male
160	+	male
160	+	male
172	+	male
64	–	femlae
65	–	femlae
74	–	femlae
94	–	femlae
123	–	femlae
129	–	femlae
138	–	femlae
160	–	femlae
161	–	femlae

[a)]Gestation day at blood sampling. [b)]Detection of SRY by nested real-time PCR. +: positive, –: negative. [c)]Phenotype of the newborn.

and SRY-3 for the second PCR is a reliable method for fetal sex determination.

Moreover, the PCR detection of circulating SRY DNA was possible at an early stage of gestation. The SRY-3 amplicon was detected from plasma samples obtained at early gestation of 42, 52, 64, or 65 days (Table 1).

Limit of detection of SRY in plasma DNA samples: Since the concentration of DNA extracted from plasma samples is too low to measure photometrically, we do not know the amount of DNA in the template sample for the 1st PCR. To avoid false-negative results due to insufficient DNA, we employed GAPDH as a guide DNA for the 1st PCR. As shown in Fig. 3, there appears to be a threshold in the copy numbers of the GAPDH amplicon, in which the SRY amplicon of the second PCR was detected or undetected. The mean copy numbers of the GAPDH amplicon were calculated to be 22,513 for positive and 838 for false-negative samples, respectively. From these data, the critical point appears to depend on the efficiency of DNA extraction from the maternal plasma samples, and the DNA level of the template should be in a range corresponding to no less than

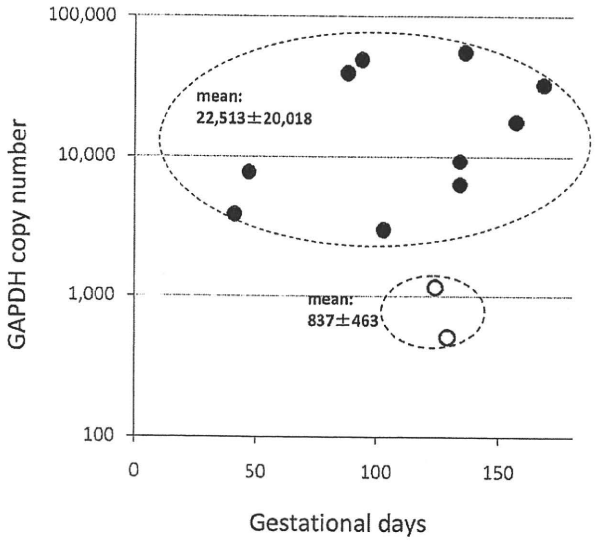

Fig. 3. The copy numbers of the GAPDH amplicon of SRY-positive (solid circles) and SRY-false-negative (open circles) samples.

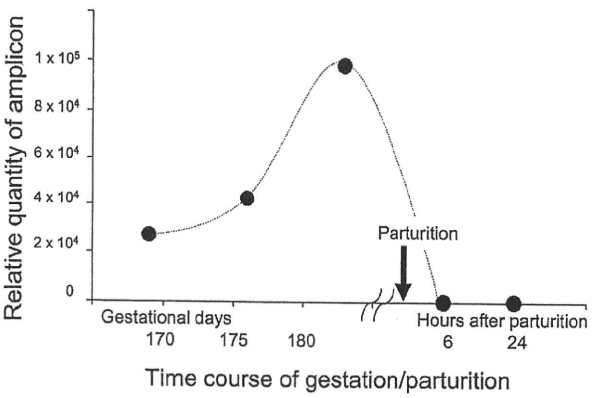

Fig. 4. Rapid clearance of fetal DNA after parturition. The relative quantity of SRY-3 amplicon obtained by the nested PCR was plotted against the time course of gestation and parturition. Fetal SRY fragment was detected in plasma DNA samples of the pregnant macaque with a male fetus. However, it was not detected in plasma samples obtained 6 or 24 h after parturition.

20,000 copies of the GAPDH amplicon.

Rapid clearance of SRY DNA from maternal plasma after delivery: To examine the clearance of fetal SRY DNA circulating in maternal blood, blood samples were obtained at term, on the day of delivery and after delivery, and subjected to SRY DNA detection. Typical results regarding the time course of circulating SRY DNA detected in maternal blood are shown in Fig. 4. No SRY

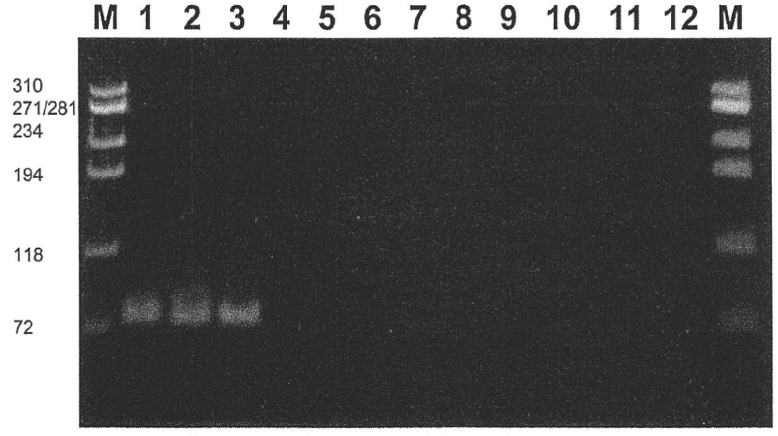

Fig. 5. SRY detection by nested PCR with a regular PCR machine. 1–9; samples of male fetus, 10–12; samples of female fetus, M; marker. Annealing for the first PCR; 1–3 and 10–11 at 63°C; 4–6 at 61°C; 7–9 at 59°C. Annealing for the second PCR; 1, 4, 7, and 10 at 63°C; 2, 5, 8, and 11 at 61°C; 3, 6, 9, and 12 at 59°C.

DNA was detected in maternal blood 6 or 24 h after delivery, indicating rapid clearance of the fetal SRY DNA from maternal circulation within 6 h after delivery.

SRY DNA detection with regular PCR machine: The present method enabled fetal sex determination by a nested PCR using a regular PCR machine. Among three annealing conditions, 63, 61, and 59°C, annealing at 63°C was effective for the first PCR, while there was no difference among the three annealing conditions for the second PCR (Fig. 5). The resulting nested PCR product gave a single band of 75 bp in PAGE, indicating that the specific SRY-3 amplicon was also amplified by this conventional nested PCR with a regular PCR machine.

Since Lo *et al.* reported the presence of fetal DNA (fDNA) in maternal plasma and serum [7], it has been used for sex determination and/or diagnosis of several fetal disorders in humans [2]. In non-human primates, fDNA in maternal plasma/serum is also an invaluable tool for determining fetal sex by non-invasive analysis coupled with PCR. Fetal sex determination is required for some biomedical studies using monkey fetuses, in which sex differences in the response to administered drug(s) or material(s) are anticipated. In a previous study, prenatal sex determination was performed to detect fetal male SRY DNA in macaque maternal serum/plasma by means of real-time PCR using the TaqMan system [5]. That method, however, needs a specific TaqMan probe and expensive apparatus to perform real-time PCR. Here we have described a method for SRY DNA detection in macaque maternal plasma by the nested PCR method, which can be performed by either real-time PCR using the SYBR Green system or conventional PCR with a regular PCR machine.

In the present study of 21 pregnant macaques, SRY DNA circulating in maternal blood was detected in all females pregnant with male fetuses, but not in any case of pregnancy with a female fetus. Moreover, PCR detection of the circulating SRY DNA was possible at an early stage (42 days of gestation). These results indicate that the current nested PCR method is highly reliable and sensitive for determining fetal sex even in the early stage of pregnancy. We employed this nested PCR method to determine fetal sex in studies of nanomaterial effects upon male or female fetus.

As the fDNA circulating in maternal blood has mostly been of concern to applied science researchers for various prenatal diagnoses, only a few studies have addressed the biological nature and tissue origin [12]. In our macaques, circulating fetal SRY DNA decreased to an undetectable level just 6 h after parturition, indicating rapid clearance from maternal blood. This observation may also indicate placental origin of the cell-free fDNA circulating in maternal plasma.

In conclusion, a nested PCR method was established for sensitive fetal sex determination in macaque monkeys. This method can be applied not only to real-time PCR using the SYBR Green system but also to conventional PCR with a regular PCR machine.

Acknowledgments

We would like to thank Dr. Ken Takeda for invaluable discussions, Dr. Kanichiro Nagatomo for technical assistance, and Dr. Elizabeth Nakajima for English correction. This work was supported in part by a Special Grant for Primate Research (820004420008 to S.N.) and Health Labour Sciences Research Grant (H20-Kagaku-Ippann-0088 to K.T).

References

1. Bayne, K. 1998. *Ann. N. Y. Acad. Sci.* 862: 105–110.
2. Chiu, R.W. and Lo, Y.M. 2002. *Expert. Rev. Mol. Diagn.* 2: 32–40.
3. Ellinwood, W.E., Stanczyk, F.Z., Lazur, J.J., and Novy, M.J. 1989. *J. Clin. Endocrinol. Metab.* 69: 348–355.
4. Jeong, A., Nakamura, S., and Mitsunaga, F. 2008. *J. Med. Primatol.* 37: 290–296.
5. Jimenez, D.F. and Tarantal, A.F. 2003. *Pediatr. Res.* 53: 18–23.
6. King, B.F. 1991. *Placenta* 12: 7–14.
7. Lo, Y.M., Corbetta, N., Chamberlain, P.F., Rai, V., Sargent, I.L., Redman, C.W., and Wainscoat, J.S. 1997. *Lancet* 350: 485–487.
8. Lo, Y.M., Tein, M.S., Lau, T.K., Haines, C.J., Leung, T.N., Poon, P.M., Wainscoat, J.S., Johnson, P.J., Chang, A.M., and Hjelm, N.M. 1998. *Am. J. Hum. Genet.* 62: 768–775.
9. Patterson, T.A., Binienda, Z.K., Newport, G.D., Lipe, G.W., Gillam, M.P., Slikker, W. Jr., and Sandberg, J.A. 2000. *Teratology* 62: 93–99.
10. Tarantal, A.F. and Hendrickx, A.G. 1988. *J. Med. Primatol.* 17: 105–112.
11. Wang, C. and Slikker, W. Jr. 2008. *Anesth. Analg.* 106: 1643–1658.
12. Wataganara, T. and Bianchi, D.W. 2004. *Ann. N. Y. Acad. Sci.* 1022: 90–99.

Review

Foods & Food Ingredients J. Jpn., Vol. 213, No.8, 2008

Assessments of Functional Foods Using Non-Human Primate Models

サルモデルを用いた機能食品の評価試験

光永　総子[a,b]　中村　伸[a]
Fusako Mitsunaga　Shin Nakamura

[a] 京都大学霊長類研究所
愛知県犬山市官林41-2
Primate Research Institute, Kyoto University
41-2, Kanrin, Inuyama-shi, Aichi 484-8506, Japan

[b] NPO法人プライメイト・アゴラ
愛知県名古屋市千種区山添町1-15
Primate Agora, NPO
1-15, Yamazoe-cho, Chikusa-ku, Nagoya-shi, Aichi 464-0832, Japan

Summary

Supply and demand of functional foods and supplements have been expanding, however knowledge regarding the efficacy and safety of these material has not been accumulated yet. Pre (or non)-clinical assessments are necessary both for the benefit of consumers' health and for biomedical and scientific progress. Monkeys are invaluable for these assessments because of their similarity in genomic, physiological, biochemical and anatomical natures with humans. Since monkey has the closest life cycle to that of human, it provides the most reliable results in biomedical research of chronic disorders associated with aging and menopause. We examined the effects of soybean functional components (β-Conglycinin and isoflavone) and inulin using post-menopause primate models (ovariectomized cynomolgus monkeys). In the soybean project, we found the efficacy of β-Conglycinin to improve hypercholesterolemia and to ameliorate osteoporosis and the action of isoflavone in the central nervous system. In another project, inulin was found to modulate intestinal microflora.

1. はじめに

人々の健康に関わる医薬品開発では前（非）臨床試験、すなわち動物を使って実験する過程が不可欠であり、安全性・有効性について調べられている。しかし、医薬品ではなく食品として取り扱われるが、やはり人々の健康を大きく左右する可能性のあるサプリメントや機能食品の安全性や有効性評価については未だ不十分なものが多い。いわゆる機能食品の中では、国に「特定保健用食品（特保）」として申請する食品のみ有効性・安全性試験を必要とするが、その他の機能食品にはそのような規制がない[1,2]。近年、ライフスタイルの変化に伴う不規則な食生活や、食餌の重要性への認識低下により、偏った食餌内容や摂取カロリー過多による健康被害の増加が危惧されている一方で、健康志向による「健康食品」ブームがあり、機能食品の市場は大きい。このような中、メーカー・販売者は、機能食品の有効性と安全性についての適切な試験を行った上、科学的根拠をもって消費者に提供すべきであろう。また、これらの試験で得られた結果は、肥満、糖尿病、高脂血症、さらにこれらが併合したメタボリックシンドロームのような慢性疾患・異常の病態解明、予防・治療に関わる重要なバイオ知見に繋がる可能性もある。

サル類（本稿では主にニホンザル、アカゲザル、カニクイザルなどマカクザル類について述べる）は図1に示すように系統的にヒトに近縁であるため、その遺伝子・ゲノム、生物学・生理学的特性がヒトに酷似している。そのため、種々の研究・試験において、ヒトに外挿可能な信頼度の高い結果を産み出すサルモデルでの前臨床試験が注目されている。

本稿では、実験動物としてのサルモデルの特徴・利点・課題、および機能食品の安全性・有効性評価試験におけるサルモデルの意義と重要性などを概説する。さらに、現在我々が進めているサルモデル（健常あるいは閉経モデル）での機能食品（ダイズ成分およびイヌリン）

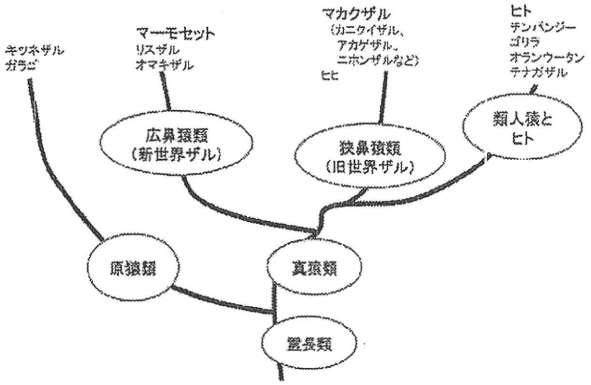

図1. 霊長類の系統樹

の評価試験について紹介する。

2. 実験動物としてのサルの特性

2-1. 実験動物として用いられる代表的なサル：マカクザルとマーモセット

ヒトを含む霊長類の系統的関係を簡単に表すと図1のようになる。ヒトはチンパンジーなどの類人猿とひとまとまりのグループに入るが、これに最も近いサル類は、アジアに生息するマカクザル（カニクイザル、アカゲザル、ニホンザルなど）とアフリカのヒヒ類を含む狭鼻猿類（旧世界ザル）である。それよりも前に分岐して南米に生息するのがマーモセットやオマキザルを含む広鼻猿類で、ユーラシア大陸に対しての新大陸（アメリカ大陸）にいるサルということで新世界ザルともよばれる。これらサル類のうち、医生物学的実験によく用いられているのはマカクザルとマーモセットである。

2-1-1. マカクザル

インドネシア、フィリピン、マレー半島など東南アジア生息のカニクイザル（体重メス3～6 kg、オス4～8 kg）、それにオーバーラップするが大陸生息のアカゲザル（体重メス4～10 kg、オス5～14 kg）、そして日本生息のニホンザル（体重メス6～10 kg、オス8～15 kg）などがいる[3]。これらマカクザルはヒトと同様の月経周期を持ち、妊娠期間は6ヶ月弱である。カニクイザルは通年繁殖するが、アカゲザル、ニホンザルは繁殖に季節性がある。寿命は長く、施設飼育では30年近く生きることもある。

2-1-2. マーモセット

南米生息でオスメスとも体重300～500 gほどしかない小型ザルである[3]。小さいためにハンドリングが容易である。1年ほどで性成熟し、妊娠期間は5ヶ月ほど、通常双子を出産し、あまり間をおかずに次の繁殖サイクルに入り、繁殖率は高い。

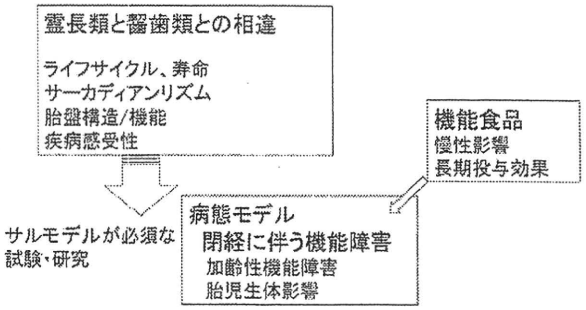

図2. バイオメディカル研究におけるサルモデルの重要性

2-2. ラット・マウスとの違い

実験動物として使われる霊長類と、ラット・マウスなど齧歯類とでは、発達速度、老化、寿命に大きな乖離があり、サル類はよりヒトに近いライフサイクルを持っている（図2）。慢性疾患の病態解明や治療・予防の研究では長期観察や治療薬の長期投与が求められる。同様に人々が日常的にしかも長期間摂取するであろう機能食品の効果や影響を調べる場合も長期投与実験が必要である。しかしながら、ラット・マウスのライフスパンは短いため、長期投与実験は困難である。これに対し、サル類は上で述べたように寿命が長く、年単位での実験が可能である。

また霊長類と齧歯類とでは生殖関連ホルモン動態や胎盤構造が異なるため、胎児が関わる試験にはサル類が必須な場合がある。霊長類と齧歯類の胎盤はともに他の哺乳類よりも母親－胎児間が密接な血絨毛胎盤である。しかし、霊長類は齧歯類とは違い、妊娠が進むにつれ母親－胎児を隔てる細胞層が融合して一層のみとなり、母親－胎児間の物質移行は密に行われる。したがって、齧歯類では母体から胎児へ移行しない物質でも、ヒトやサルでは移行し易くなる。母親が摂取した物質が胎児に重大な影響を及ぼした症例のうち、齧歯類での試験では異常が認められず、霊長類を使ってはじめてヒトと同じ結果が得られたものに「サリドマイド奇形」がある[4]。このように母体に投与された物質の胎児への影響を調べるにはサル類が必要である[5]。

サル類はラット・マウスのように実験動物として確立された純系の系統はない。そのため、サルでの試験はラ

ット・マウスでの試験よりも個体差が大きく出るのが普通である。ラット・マウスの単一ストレイン内で多くの個体を用い、狭い範囲内に個体差が納まったとしても、それらの動物は単一に確立された系であるから、その動物集団は極端な場合、ヒトやサルの一個体にしか相当しないと言える。ヒトでは当然個体差が出る。個体差は試験での評価を難しくするが、ヒトへの適用を見据えれば、サルでの試験で個体差が出た理由とメカニズムを解明することは有用であろう。

3. サルを使った評価系での課題と対策

3-1. 飼育・実験にかかる費用と労力

実験動物として使われるサルの値段は通常数十万円とかなり高価である。またマカクザルは体が大きいのでそれに見合う大きさのケージが必要である。サルの飼育・実験施設を持つ研究所や事業所はそれぞれ、ケージの大きさをはじめとする飼育条件や実験方法についてのガイドラインを持ち、それに従っている。これらのガイドラインはアメリカのNational Research Councilによるガイドラインをベースにしたものである[6]。動物福祉の観点からも、試験の質を保証するためにもこれらガイドラインは遵守されている。このように、サルの飼育・実験には費用、設備、人手を要するので、サル試験の可能な施設が限られる。また、ひとつの試験に使える個体数も制限される。したがって、試験ひとつひとつについて、サルで行う必要性について熟考した上で、必要数と実験デザインについて吟味しなければならない。ラット・マウスなど汎用実験動物での試験がヒトに外挿できる場合はそれらを使用する。むやみに多数の個体を使用するのではなく、意味のある解析ができる最小限動物数での実験デザインを組む努力をする。また、同一個体を多重利用し有効活用すべきである。

3-2. 人獣共通感染症

サルはヒトに近いため、宿主特異性の高いウイルスなどでも共通に感染することがある。中でもサル類実験動物施設で問題になるのはマカクザルを自然宿主とするBウイルスである。このウイルスはヒトの単純ヘルペスウイルスと同じ仲間で、マカクザルでの感染は通常不顕性であるが、これまでに報告されたヒトへの感染では致死率80%前後の重篤な中枢神経系障害を起こしている[7,8]。単純ヘルペスと同様に口腔や生殖器に感染性ウイルスが排出されることがあるので、Bウイルス陽性サルに噛まれたり、唾液や排泄物に曝露されたりしないよう物理的に防護した上で注意しなければならない。

実験施設のマカクザルBウイルス感染症は隔離プログラムと抗体モニタリングとでコントロールできるので、むやみに恐れて過剰反応を示すのはよくない。抗体検査に使う抗原としては、増殖に特別な設備を必要とするBウイルスそのものでなくても、これと交差性の高い代替抗原（ヒヒのヘルペスウイルス：HVP2やミドリザルのヘルペスウイルス：SA8など）が使える[9,10]。これら代替抗原を活用し、十分頻繁な抗体検査を実施するのが得策である。我々はHVP2を代替抗原とした高感度なELISA法を確立し、定期的にBウイルス抗体検査を行っている[11]。

3-3. 動物愛護/アニマルライトへの配慮・対応

動物実験に反対する動物愛護団体もあり、特にサルを使った試験・研究はそれだけで非難されるかもしれない。この場合重要なのは、その試験・研究をサルで行うことの必要性と意義を明らかにして、社会に示すことであろう。動物愛護団体のみならず、社会一般に対して「なぜサルで実験しなければならないのか」を発信する。また攻撃を恐れて実験内容を隠そうとすればかえって誤解を招きかねない。実験内容について説明し、理解を得られるよう情報公開など心掛けるべきであろう。サルを実験に使う側は常にそれぞれの試験の意義を見極め、無駄のない最適な実験計画で研究・試験を実施する必要がある。

4. サルモデルでの機能食品評価試験

4-1. ダイズ成分（イソフラボン、ベータコングリシニン）の評価試験の概要

4-1-1. 背景・目的

図3に示すように、これまで加齢性機能障害/閉経に伴う①脂質代謝異常（高脂血症）および②骨代謝異常（骨粗鬆症）に対するダイズ成分の効果と作用機序について解析を進め、ダイズタンパク質（β-Conglycinin, β-CG）の新たな機能として骨粗鬆症改善作用を見出した[12~14]。

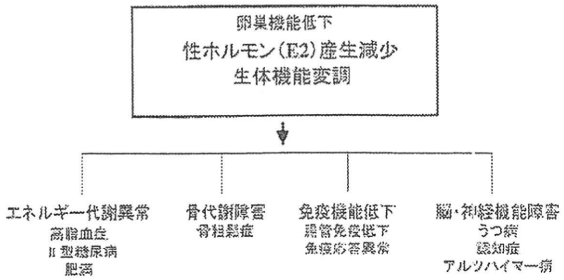

図3. 加齢性機能障害（閉経性機能障害）

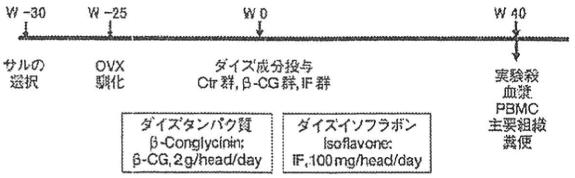

図4. カニクイザルモデルでの実験計画

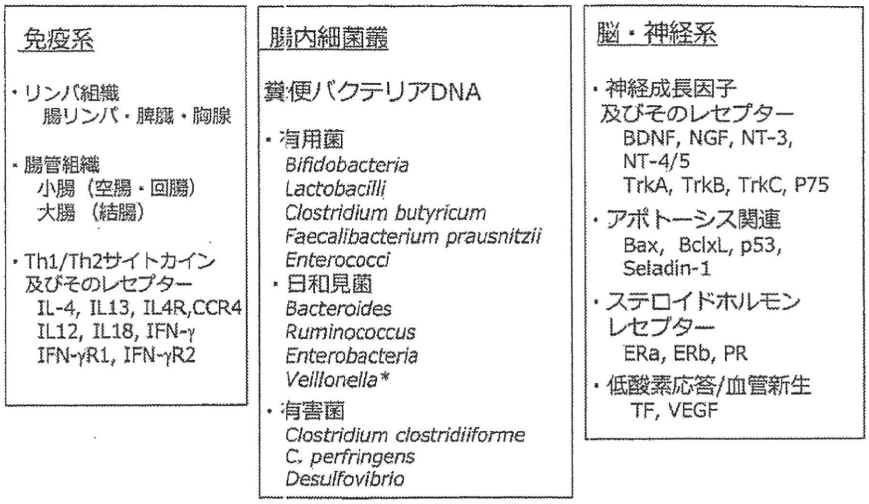

図5. 免疫系・腸内細菌叢・脳神経系のゲノム・遺伝子解析
＊Veillonellaは有害菌とされることが多いが、後述のように病原菌抑制の報告もあるため、ここでは便宜的に日和見菌に入れる。

一方、ダイズイソフラボン（Isoflavone, IF）では、高脂血症および骨粗鬆症のいずれに対しても改善作用は認められず、従来のラット・マウスでの試験結果とは異なっていた[15, 16]。さらに、この閉経カニクイザルモデルを活用して、③免疫応答系、④脳・神経系に対するβ-CGあるいはIFの影響・効果を、主にゲノム・機能遺伝子レベルでの発現プロファイル解析を通じて評価検討した。また、⑤アレルギー抗原性についても安全性の視点から検討した。

4-1-2. 材料・方法

(a) サル閉経モデルへのダイズ成分の投与

本研究では、成体メスのカニクイザルを卵巣摘出（Ovariectomy, OVX）して作出したOVX-閉経サルモデルを用いた。これらのOVX-閉経サルモデルに、被検物質としてβ-CGあるいはIFを、ヒトでの摂取量に近い2.0 g/head/day（β-CG）、100 mg/head/day（IF）を、図4に示すように長期連続経口投与し、以下の試験を実施した。

(b) 遺伝子発現・ゲノム解析

コントロール（Ctr）群、β-CG投与群およびIF投与群について、それぞれの主要リンパ組織および脳各部位を採取後、種々組織試料から既報[13]に従ってDNAフリーの高純度RNAを調製した。得られたRNAを用いOligo-dT primerでのRT反応後、図5に示す機能遺伝子の特異的PCRプライマーを用いたReal Time Reverse Transcriptase-PCR 法（リアルタイムRT-PCR法）を実施し、機能遺伝子群の発現変動を定量解析した。さらに、糞便試料についてはQIAGENのstool kitを活用して、糞便中の腸内細菌DNAを抽出し、腸内細菌に対する特異的PCRプライマー（表1）を用いたReal Time PCR法（リアルタイムPCR法）で腸内細菌叢の動態を定量比較した。

4-1-3. 評価試験結果の要約

本試験研究では、閉経性機能障害サルモデルを作出し、コレステロール・脂質代謝、骨代謝、免疫応答能、腸内細菌フローラおよび脳神経機能に対する、ダイズ主成分のβ-CGおよびIFの障害予防・改善作用について、遺伝

子・ゲノムレベルで解析し、図6に示すような結果を得た。

閉経サルモデルを利用した本研究を通じてβ-CGによる骨密度低下抑制（骨粗鬆症改善）作用が初めて明らかにされ、β-CGおよびそのペプチド成分を利用した骨粗鬆症用の新たな機能食品・サプリメントの誕生に繋がる知見を得た[12~14]。

また、免疫応答に関しては、IFが脾臓および胸腺でのTh1/Th2応答関連遺伝子群の発現抑制を示すことから、IFが細胞性・液性免疫応答を制御する可能性が窺える[20]。さらに、腸内細菌ではIF投与群に日和見菌群の菌数著減が見られ、IFが腸内細菌フローラや腸内環境に強く影響することが示唆された[20]。加えて、脳神経機能への影響では非常に興味深い知見が得られた。閉経後に機能低下が予測されている海馬や大脳皮質（前頭葉）において、IFは強いERa遺伝子発現亢進作用を示し、これら認知・行動の主要部位におけるERa発現・生成促進を介して、閉経後の認知・行動の機能低下をIFが改善していることが明らかにされた[20]。また、運動機能に関わる小脳において、IFが神経成長因子のNT-3およびNT-4/5遺伝子の発現を強く抑制することから、IFが閉経後の小脳機能をモジュレートすることも示唆された[20]。

表1. リアルタイムPCR法で定量測定した細菌

プライマー略号	対象細菌	文献
Bif	*Bifidobacterium* spp.	17)
Lacto	*Lactobacillus* group	17)
Cbu	*Clostridium butyricum*	18)
Fpr	*Faecalibacterium prausnitzii*	18)
Efs	*Enterococcus* spp.	17)
Bac	*Bacteroides-Prevotella* group	18)
Ral	*Ruminococcus albus*	18)
Eco	*Enterobacteriaceae*	18)
Veillo	*Veillonella* spp.	17)
Ccl	*Clostridium clostridiiforme*	18)
Cpe	*Clostridium perfringens* group	17)
Dsv	*Desulfovibrio* genus	18)
Uni	(Universal probe)	19)

各細菌（グループ）の16S-rRNA遺伝子の特異的配列部分を増幅し定量した。各細菌DNAの量はユニバーサルなプライマー（Uni）で増幅したDNA量に対する比として算出した。

4-2. イヌリンの評価試験の概要

4-2-1. 背景

イヌリンはキクイモやチコリなどに多く含まれる水溶性食物繊維で、その構造はβ1→2グリコシド結合でつながるフルクトースのポリマー（通常末端にグルコース）である[21]。ヒトや動物にはこの結合を切る酵素がないので、小腸ではイヌリンは消化されないが、腸内細菌、特にBifidobacteriaやLactobacilliなどの乳酸菌がイヌリンを利用し、分解する[22]。この性質によりイヌリンは整腸作用をはじめ、血糖上昇抑制作用やミネラル吸収促進作用などを持つと報告されているため[23]、老化や閉経に伴うメタボリックシンドロームや骨粗鬆症に対する改善・緩和作用が期待される。しかしながら、これまでの報告は主にラット・マウスを使用した実験によるもので、ヒトの加齢・閉経状態を近似できる霊長類モデルでイヌリンを長期間投与した試験はない。我々はヒトに近い生殖関連ホルモン動態を持つマカクザルで閉経モデルをつくり、イヌリンが腸内細菌叢、脂質代謝、糖代謝、骨代謝に及ぼす影響を調べている。今回は主に腸内細菌叢の変

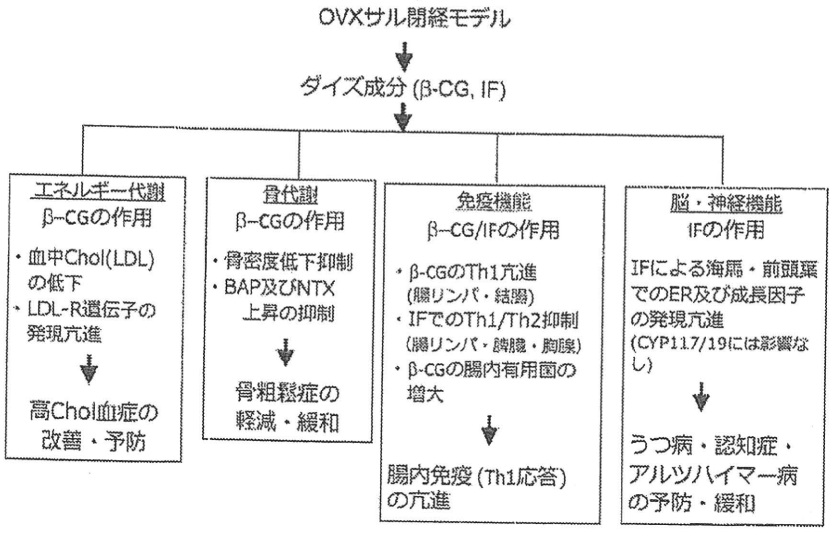

図6. ダイズ成分（β-CG, IF）による加齢性機能障害（閉経性機能障害）の緩和・改善作用とその分子機序

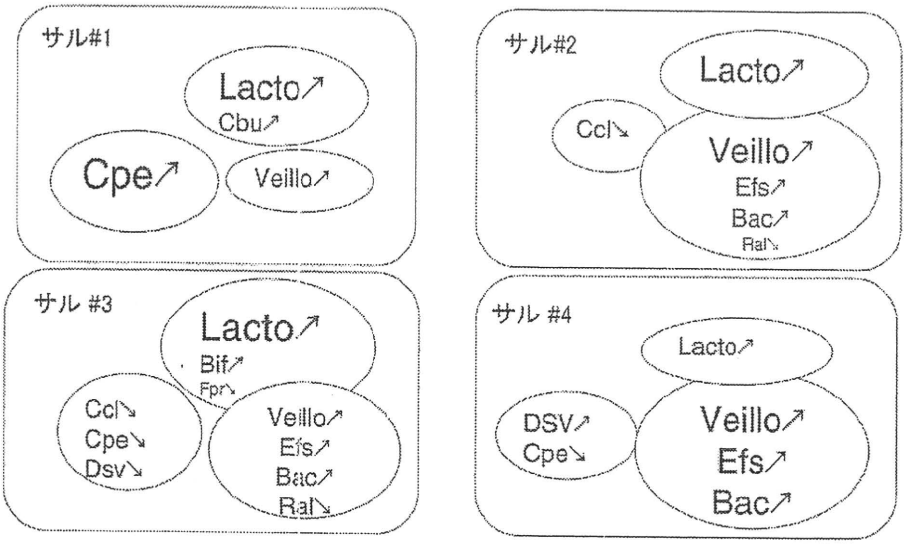

図7. イヌリンの腸内細菌叢への影響（3倍以上の増加：↗、1/3以下の減少：↘）
視覚的にイメージし易いように、細菌の増減の度合いに応じて字の大きさを変えてある。

動について紹介する。

4-2-2. 方法

メスカニクイザル4頭より卵巣除去し、閉経モデルを作成した。馴化期間後、ヒトの日常的摂取量に換算した量のイヌリン（2.0 g/head/day）を3ヶ月間毎日経口投与し、経時的に糞便を採取した。「4-1.ダイズ成分の評価試験」と同様に、糞便サンプル中の代表的な腸内細菌のDNA量をリアルタイムPCR法で定量測定した（表1）。

4-2-3. 結果と考察

イヌリン投与前の糞便中細菌DNA量には個体によるばらつきが見られた。特に今回着目すべき細菌について、表2に各個体の投与前細菌DNA量を示した。サル#1のように、もともとBacteroidesのような日和見菌が多く、BifidobacteriaやLactobacilliのような乳酸菌が少ない個体がいるのがわかった。

3ヶ月のイヌリン連続経口投与の結果、これまで報告されていたように、Bifidobacteriaの増加は今回の実験でも認められ、個体によって投与開始後1ヶ月、あるいは2ヶ月後にピークがあった。しかしながら3ヶ月間の投与終了時点では、Bifidobacteriaの量は結果的に殆ど投与前のレベルに戻っていた。イヌリン投与開始前と3ヶ月連続投与後の腸内細菌叢を比較し、最終的に増減が認められた細菌をまとめると図7のようになる。全ての個体においてLactobacilliとVeillonellaの増加が見られた。これまで、ヒトの短期摂取実験や*in vitro*実験ではLactobacilli

表2. イヌリン投与前の糞便中細菌DNA相対量

プライマー略号	*Uniに対する比×10⁸			
	サル#1	サル#2	サル#3	サル#4
Bif	33	1479	105	109
Lacto	562	561022	8972	37327
Bac	2172286	308488	80043	4377
Veillo	4	112	86	828
Cpe	211	25420	55373	32625

*：今回特に着目した細菌の特異的プライマーで検出したDNA量を、ユニバーサルプライマーによるDNA量で割ったもの。見やすくするために、10⁸倍してある。

の増加よりもBifidobacteriaの増加が大きいことが報告されていたが[24,25]、そこでは投与（実験）期間が短かったために、長期摂取の影響が捉えられなかったのかもしれない。また、老化に伴い、BifidobacteriaよりもLactobacilliが多くなるという報告[26]と一致して、今回使用したサルモデルはもともとLactobacilliの方が多かったことから（表2）、我々の試験はヒトにおける「老齢で閉経」という状態をよく近似していると思われる。

Veillonellaは乳酸菌がイヌリンを分解して産生した乳酸を利用して増えた可能性がある。感染症が報告されているためにVeillonellaは有害菌に区分されることが多いが、常在菌としてサルモネラ等の病原菌感染を抑制するとの報告もあり[27]、その性質はまだよくわかっていない。

サルのうち、1頭は有害菌の*Clostridium perfringens*（Cpe）が増加していた。Cpeはグルコースを利用し[28]、酸性環境下でもかなり耐性であるので[29]、イヌリン投与で乳酸菌が増えた状態でも増加する可能性はある。この個体は他個体と比較すると、投与前よりCpeも少なかっ

たがBifidobacteriaやLactobacilliも少なかった（表2）。このような場合、プロバイオティクスとの組合せ投与が腸内細菌叢の改善により有効かもしれず、今後の課題である。これらのことから、機能食品のヒトへの適用において投与前および投与期間中の腸内細菌叢をモニターする意義が示唆された。

5. まとめ

昨今、機能食品の需要・供給がますます増大しつつあるが、機能食品の有効性・安全性については適切な試験を行い、科学的根拠をもって消費者に提供すべきである。サル類はヒトに類似のライフサイクルや生理学的な特性を持つので、機能食品試験においても他の動物には取って代われない有用なモデルとなる。ただ、サルの実験・飼育には大きな費用、労力がかかるので、サルを使える実験施設は限られる。また、試験に使用するサル個体数は制限されるので、科学的にも充分に洗練された試験を行う必然性が出てくる。動物福祉という観点からも、実験デザインの最適化に努め、意義のある試験を行う必要がある。

引用文献

1) 林浩孝, 大野智, 太田康之, 新井隆成, 鈴木信孝, 特定保健用食品の許認可について, 日本補完代替医療学会誌, 4, 103-112 (2007).
2) 保健機能食品制度, 厚生労働省, URL: http://www.mhlw.go.jp/topics/2002/03/tp0313-2a.html
3) 杉山幸丸ら, "サルの百科", データハウス, 1996.
4) L. M. Newman, E. M. Johnson and R. E. Staples, Assessment of the effectiveness of animal developmental toxicity testing for human safety, *Reprod. Toxicol.*, 7, 359-390 (1993).
5) M. Hirano, S. Nakamura, F. Mitsunaga, M. Okada, K. Shimizu and T. Imamura, Transfer of maternally administered fusogenic liposome-DNA complexes into monkey fetuses in a pregnancy model, *J. Gene Med.*, 4, 560-566 (2002).
6) National Research Council, "Guide for the care and use of laboratory animals", National Academy Press, Washington, DC, 1996.
7) 中村志帆, 光永総子, 中村伸, サルの安全な取扱いのために－感染リスクの対応手引き, 霊長類研究, 15, 337-394 (1999).
8) 光永総子, 藤本浩二, 中村伸, Bウイルス (*Cercopithecine herpesvirus* 1) 感染の予防, 緊急対応および治療に関するガイドライン, 霊長類研究, 20, 147-164 (2004).
9) K. Ohsawa, T. W. Lehenbauer and R. Eberle, *Herpesvirus papio* 2: alternative antigen for use in monkey B virus diagnostic assays, *Lab. Anim. Sci.*, 49, 605-616 (1999).
10) J. Takano, T. Narita, K. Fujimoto, R. Mukai and A. Yamada, Detection of B virus infection in cynomolgus monkeys by ELISA using simian agent 8 as alternative antigen, *Exp. Anim.*, 50, 345-347 (2001).
11) F. Mitsunaga, S. Nakamura, T. Hayashi and R. Eberle, Changes in the titer of anti-B virus antibody in captive macaques (*Macaca fuscata, M. mulatta, M. fascicularis*), *Comp. Med.*, 57, 120-124 (2007).
12) 中村伸, 光永総子, 山内英典, 岡田真紀, Aram Joeng, 林隆志, Rosalio M. Perez, Romualdo L. Carrasco, 中川博司, ダイズ成分による高脂血症および動脈硬化への予防・治療効果の作用機序：サルモデルを用いた分子病態生理学的研究, 大豆たん白質研究, 6, 57-62 (2003).
13) 中村伸, 光永総子, 山内英典, Aram Joeng, 林隆志, Joseph Gabriel, ダイズ食品・成分による加齢性機能障害および生活習慣病の予防作用：サルモデルでのゲノム医生物学的研究(I), 大豆たん白質研究, 7, 13-19 (2004).
14) 中村伸, 光永総子, A-Ram Joeng, 山内英典, 林隆志, Joseph Gebriel, 大豆食品・成分による加齢性機能障害および生活習慣病の予防効果：サルモデルでのゲノム医生物学的研究(II), 大豆たん白質研究, 8, 1-7 (2005).
15) E. A. Lucas, S. A. Lightfoot, L. J. Hammond, L. Devareddy, D. A. Khalil, B. P. Daggy, Y. Soungdo and B. H. Arjmandi, Soy isoflavones prevent ovariectomy-induced atherosclerotic lesions in Golden Syrian hamster model of postmenopausal hyperlipidemia, *Menopause*, 10, 314-321 (2003).
16) T. Uesugi, T. Toda, K. Tsuji and H. Ishida, Comparative study on reduction of bone loss and lipid metabolism abnormality in ovariectomized rats by soy isoflavones, daidzin, genistin, and glycitin, *Biol. Pharm. Bull.*, 24, 368-372 (2001).
17) T. Rinttilä, A. Kassinen, E. Malinen, L. Krogius and A. Palva, Development of an extensive set of 16S rDNA-targeted primers for quantification of pathogenic and indigenous bacteria in faecal samples by real-time PCR, *J. Appl. Microbiol.*, 97, 1166-1177 (2004).
18) S. Bartosch, A. Fite, G. T. Macfarlane and M. E. McMurdo, Characterization of bacterial communities in feces from healthy elderly volunteers and hospitalized elderly patients by using real-time PCR and effects of antibiotic treatment on the fecal microbiota, *Appl. Environ. Microbiol.*, 70, 3575-3581 (2004).
19) M. A. Nadkarni, F. E. Martin, N. A. Jacques and N. Hunter, Determination of bacterial load by real-time PCR using a broad-range (universal) probe and primers set, *Microbiology*, 148 (Pt 1), 257-266 (2002).
20) 中村伸, 光永総子, 橋本寛之, 出井早苗, 林隆志, Joseph Gabriel, 大豆食品・成分による閉経性/加齢性機能障害の予防作用：サルモデルでのゲノム医生物学的研究(III), 大豆たん白質研究, 9, 1-8 (2006).
21) T. M. Calub, A. L. Waterhouse and A. D. French, Conformational analysis of inulobiose by molecular mechanics, *Carbohydr. Res.*, 207, 221-235 (1990).
22) K. R. Niness, Inulin and oligofructose: What are They?, *J. Nutr.*, 129, 1402S-1406S (1999).
23) M. B. Roberfroid, Introducing inulin-type fructans, *Br. J. Nutr.*, 93, S13-25 (2005).
24) B. Kleessen, B. Svkura, H. -J. Zunft and M. Blaut, Effects of

inulin and lactose on fecal microflora, microbial activity, and bowel habit in elderly constipated persons, *Am. J. Clin. Nutr.*, **65**, 1397-1402 (1997).
25) Y. Bouhnik, L. Raskine, K. Champion, C. Andrieux, S. Penven, H. Jacobs and G. Simoneau, Prolonged administration of low-dose inulin stimulates the growth of bifidobacteria in humans, *Nutr. Res.*, **27**, 187-193 (2007).
26) M. J. Hopkins and G. T. Macfarlane, Changes in predominant bacterial populations in human faeces with age and with Clostridium difficile infection, *J. Med. Microbiol.*, **51**, 448-454 (2002).
27) A. Hinton Jr. and M. E. Hume, Antibacterial activity of the metabolic by-products of a Veillonella species and Bacteroides fragilis, *Anaerobe*, **1**, 121-127 (1995).
28) M. Egert, A. A. de Graaf, A. Maathuis, P. de Waard, C. M. Plugge, H. Smidt, N. E. P. Deutz, C. Dijkema, W. M. de Vos and K. Venema, Identification of glucose-fermenting bacteria present in an in vitro model of the human intestine by RNA-stable isotope probing, *FEMS Microbiol. Ecol.*, **60**, 126-135 (2007).
29) P. D. Cotter and C. Hill, Surviving the acid test: Responses of gram-positive bacteria to low pH, *Microbiol. Mol. Biol. Rev.*, **67**, 429-453 (2003).

PROFILE

光永　総子
京都大学霊長類研究所
教務補佐員
獣医学修士

1986年北海道大学大学院獣医学研究科予防治療学専攻修士課程修了、同年京都大学霊長類研究所研修員、1997年同研究支援推進員、2006年NPO法人プライメイト・アゴラ監事。

中村　伸
京都大学霊長類研究所
助教
東京理科大学
客員教授
理学博士